Arabian Journal of Chemistry (2021) **14**, 103022

King Saud University

Arabian Journal of Chemistry

www.ksu.edu.sa
www.sciencedirect.com

ORIGINAL ARTICLE

Surface charge on chitosan/cellulose nanowhiskers composite via functionalized and untreated carbon nanotube

Chin Zhen Thou [a], Fahad Saleem Ahmed Khan [a], N.M. Mubarak [a,*], Awais Ahmad [b], Mohammad Khalid [c], Priyanka Jagadish [c], Rashmi Walvekar [d], E.C. Abdullah [e], Safia Khan [f], Mariam Khan [g], Shahid Hussain [h,*], Ikram Ahmad [i,*], Tahani Saad Algarni [j]

[a] *Department of Chemical Engineering, Faculty of Engineering and Science, Curtin University, 98009 Miri, Sarawak, Malaysia*
[b] *Department of Chemistry, The University of Lahore, Lahore 54590, Pakistan*
[c] *Graphene & Advanced 2D Materials Research Group (GAMRG), School of Engineering and Technology, Sunway University, No. 5, Jalan Universiti, Bandar Sunway, 47500 Petaling Jaya, Selangor, Malaysia*
[d] *Department of Chemical Engineering, School of Energy and Chemical Engineering Xiamen University Malaysia, Jalan Sunsuria, Bandar Sunsuria, Sepang 43900, Selangor, Malaysia*
[e] *Department of Chemical Process Engineering, Malaysia-Japan International Institute of Technology (MJIIT), Universiti Teknologi Malaysia (UTM), Jalan Sultan Yahya Petra, 54100 Kuala Lumpur, Malaysia*
[f] *Department of Chemistry, Quaid-I-Azam University, Islamabad, Pakistan*
[g] *Department of Applied Sciences and Humanity (NUSASH), National University of Technology, Islamabad, Pakistan*
[h] *School of Materials Science and Engineering, Jiangsu University, Zhenjiang 212013, China*
[i] *Department of Chemistry, The University of Sahiwal, Sahiwal 54000, Pakistan*
[j] *Chemistry Department, College of Science, King Saud University, Riyadh 11451, Saudi Arabia*

Received 30 November 2020; accepted 15 January 2021
Available online 28 January 2021

KEYWORDS

Chitosan;
Cellulose nanowhiskers (CNWs);

Abstract Improvement in chitosan (CS) was achieved by solution casting using cellulose nanowhiskers (CNWs) and multiwall carbon nanotubes (MWCNTs) to synthesize CS/CNW functionalized/treated MWCNTs (CS/CNWs/f-MWCNTs) and CS/CNW untreated MWCNTs (CS/CNWs/Un-MWCNTs) nanocomposite films. A comparison between effects of f-MWCNTs and Un-

* Corresponding authors.

E-mail addresses: mubarak.mujawar@curtin.edu.my, mubarak.yaseen@gmail.com (N.M. Mubarak), shahid@ujs.edu.cn (S. Hussain), drikramahmad@uosahiwal.edu.pk (I. Ahmad).

Peer review under responsibility of King Saud University.

Production and hosting by Elsevier

https://doi.org/10.1016/j.arabjc.2021.103022

Carbon nanotubes (CNTs);
Multi-walled carbon nanotubes (MWCNTs);
Solution casting;
Nanocomposite films

MWCNTs on CS/CNWs matrix have been studied with respect to change in their physical and mechanical properties. The surface morphology, chemical composition, mechanical properties and temperature decomposition of CS/CNWs/f-MWCNTs and CS/CNW/Un-MWCNTs nanocomposite films were characterized by Energy Dispersion Spectroscopy (EDS), Field Emission Scanning Electron Microscope (FESEM), Fourier-Transform Infrared Spectroscopy (FTIR) and Thermogravimetric Analysis (TGA). FESEM has shown that f-MWCNTs and Un-MWCNTs were well dispersed in CS/CNWs structure. Decrease in film ductility was observed with addition of Un-MWCNTs or f-MWCNTs. Moreover, Tensile strength (TS) and Young's modulus (YM) were increased with f-MWCNTs and seemed to be decreased in case of Un-MWCNTs. However, a decrease in elongation at break (EB) has experienced with addition of f-MWCNTs and Un-MWCNTs. Furthermore, thermal stability of chitosan composites presented a delay or prevention from degradation of CS/CNWs due to the strong interactions. Such modification in chitosan can improve its mechanical and surface properties. Hence, chitosan derived composites could achieve more applicability in packaging, medicinal and environmental applications.

1. Introduction

Biodegradable natural polymers have gained a huge consideration as appropriate substitute of the man-made petroleum based products (Asghari et al., 2017; Wróblewska-Krepsztul et al., 2018). Chitosan (CS), a derivative of the second most abundant natural polymer chitin, and its composites have attained a massive attention owing to their low toxicity, biodegradability, bioactivity, biocompatibility and no antigenicity (Kashif et al., 2020; Ahmad et al., 2020). That's why, chitosan derivatives are widely applied in medicine, food additives, antimicrobial agents, textiles, adhesives and polluted water treatment (Zhang et al., 2020; Aravind et al., 2020). Also, such purely CS based matrices can easily be tuned into different shapes like fibers, gels, films, sponges, membranes and tubes (Hussain et al., 2020). However, some drawbacks experienced by chitosan like lower stability, less porosity, weak mechanical resistance, distribution of co-monomers and difficulty in pore size control lead to narrowing down its applicability to limited fields (Saleem et al., 2020; Naseem et al., 2020). So, the central dogma is actually the tackling of such undesirable features which can be achieved by modifications in chitosan composition. This improvement usually involves the blending of CS with some carbonaceous materials of high mechanical significance (Zhan et al., 2020; Kashif et al., 2020). Consequently, several polymers have been frequently used to blend with CS e.g. polyvinyl alcohol, polyaniline, polyvinyl pyrrolidone, starch, cellulose and their derivatives to obtain a matrix of desired physical properties (Kausar, 2017; HPS et al., 2016).

Cellulose Nanowhiskers (CNWs), generated from plant sources, act as an appropriate filler and offer high surface to volume ratio to a composite (Ahmad et al., 2020). CNWs in combination with CS could present a desired nanometer size, commendable mechanical strength, efficient electrical as well as thermal conductivity (Bao et al., 2018; Li et al., 2015). CNWs must be finely dispersed in the CS to gain maximum possible interfacial properties. CS/CNWs composite display high performance output and multiple functions due to achievement of maximum reinforcing potential (Melo et al., 2018). But, CNWs form bundles or agglomerates due to van der Waals interactions and its exceptional characteristics can't be fully expressed in a composite. Therefore, a more advanced and efficient strategy is needed to attain substantial electronic and mechanical properties to improve functioning of this matrix in a variety of applications. Purposely, some tricomponent combinations are being developed in recent years exhibiting improved biocompatibility and enhanced physical characteristics with respect to industrial and biomedical applications (Abou El-Ela et al., 2020; Kijeńska et al., 2016).

In this way, the addition of multiwalled carbon nanotubes (MWCNTs) can be an outstanding approach to increase the mechanical significance of CS/CNWs composite towards multiple functions (Thakur and Voicu, 2016). MWCNTs, as discovered by Sumio Iijima in 1991, behave as an electron reservoir in CS/CNW/MWCNT composite offering a wide range of thermal and structural properties (Shi et al., 1999). Synergistic effects appearing between MWCNTs and CS/CNW structures which can further enhance the mechanical stability of the tricomponent material. Addition of MWCNTs to CS/CNWs matrix can reduce its surface roughness, facilitates its crystallization and increases the thermal degradation temperature even without change in its degradation behavior. Chitosan/MWCNTs composite is already being applied in multitude of industrial, environmental and biomedical fields. It is used in substitutes of bones, DNA biosensors, metal removal from aqueous solutions and biofuels.

Moreover, a more comprehensive understanding of stability and strength could be attained by incorporation two different types of MWCNTs i.e. functionalized/treated MWCNTs (f-MWCNTs) and untreated MWCNTs (un-MWCNTs) into CS/CNW combination. While, f-MWCNTs possess significantly enhanced mechanical and thermal properties as compared to un-MWCNTs.

Herein, modifications in CS structure are accomplished by addition of CNWs, f-MWCNTs and un-MWCNTs to CS matrix by solution casting method to obtain some desired physical properties to make a perfect use of a naturally abundant polymer. These amendments are evaluated through different analytical methods including SEM, FTIR, TGA and EDS techniques. Besides, the improved physical parameters like thermal stability, (EB) and TS and YM are also estimated in the current research.

2. Materials and method

2.1. Raw materials

Chitosan (CS), powder of low molecular weight (50,000–190, 000 Da) exhibiting sufficient potential and more solubility, microcrystalline cellulose (MCC), acetic acid 98%, lithium chloride (LiCl), N, N dimethyl acetamide solution (DMAc) and sodium hydroxide (NaOH) purchased from Sigma-Aldrich were used as received without further purification. Un-MWCNTs with a purity of 98% and diameter range between 16 and 23 nm were synthesized according to Mubarak, Sahu (Mubarak et al., 2014) and f-MWCNTs from Jun, Mubarak (Jun et al., 2018).

2.2. Preparation of cellulose nanowhiskers (CNWs)

CNWs were prepared with MCC via chemical swelling technique and then followed by ultrasonic treatment Oksman, Mathew (Oksman et al., 2006). DMAc and 0.5% LiCl solution was used as a swelling agent. DMAc/LiCl-0.5% mixture was kept on stirring by using magnetic stirrer for 15 min. The concentration of MCC in DMAc/LiCl mixture was maintained as 10 wt%. A weighed amount of MCC powder was gently poured into DMAc/LiCl mixture while continuously agitated for 12 hrs. at 70 °C using magnetic stirrer. Afterwards, slightly swelled particles were transferred to a centrifuge bottle and centrifugation was repeated three times with the speed of 3000 RCF for 3 min. After every centrifuge cycle, supernatant was removed and replaced with distilled water. Subsequently, the suspensions were ultrasonicated for 10 min to obtain the product CNWs. Repeatedly, gel-like suspension was washed with distilled water and stored in an airtight container and refrigerated.

2.3. Preparation of CS/CNWs/MWCNTs nanocomposites

The CS/CNWs/MWCNTs composite was synthesized via solution casting processing method. The 0.5 wt% MWCNTs (both functionalized and treated MWCNTs in separate reactions) were added into 1% of the acetic acid solution and undergo dispersion by ultra-sonication bath for 1 h. After that, 2 wt % of chitosan powder was added into the solution. The mixture was stirred for 90 min at 50 °C to dissolve the chitosan powder and to form a homogeneous mixture. 5 wt% of CNWs were poured into the mixture and then stirred for 12 hrs. or more until a completely homogeneous mixture was formed. The mixture was then left at room temperature for 30 min until the air bubbles disappeared followed by ultra-sonication for 20 min to deeply remove the remaining air bubbles. The homogeneous mixture was casted into a petri dish and get evaporated at room temperature for 48 hrs. or more until a dry nanocomposite film was obtained. In order to speed up the evaporation process, the samples were placed in the fume hood. After the sample got completely dry, film was immersed in a 2% (w/v) sodium hydroxide for 20 min and then neutralized with the acetic acid and then washed thrice with distilled water. Nanocomposite film was easily removed from petri dish with the aid of NaOH. The prepared nanocomposites films were then dried at room temperature to remove the residues of water. All the samples were kept in a zip bag to avoid contact with air moisture [Fig. 1].

2.4. Characterizations

The samples with different concentrations of *f*-MWCNTs or untreated MWCNTs on Cs/CNWs were prior prepared for testing. The characterization studies would analyze their surface morphology, chemical composition, mechanical properties, and temperature decomposition, with Energy-dispersion X-ray Spectroscopy (EDX), Field Emission Scanning Electron Microscope (FESEM), Fourier-Transform Infrared Spectroscopy (FTIR), Mechanical Properties testing and Thermogravimetric Analysis (TGA). The morphology of the samples was examined by using a Field Emission Scanning Electron Microscope (FESEM, FEI Quanta 400) and Energy-dispersion X-ray Spectroscopy (EDX). For FESEM examination, samples were prepared by placing small pieces of sample films on the sample holder i.e. SEM's stage using a conductive carbon-tape. Each small piece of sample film was coated with an ultra-thin gold (Au) layer for a minimum of 100 s using an ion-sputtering machine 108 Auto Sputter Coater). Furthermore, the chemical composition was analyzed with Energy-dispersion X-ray Spectroscopy (EDX). The Fourier-transform infrared (FTIR) transmission spectra were performed with Perkin Elmer 1600 Series in ATR mode to characterize and evaluate the surface structure of nanocomposite samples. The samples were placed on an optic window with a diamond crystal. For better contact between the crystal and sample, the pressure of the applicator was maintained with the help of a pressure control spot. After each measurement, both the anvil of the pressure applicator and the crystal plate was cleaned thoroughly. The tensile strength properties were analyzed based on ASTM standard (D-3822) using an INSTRON Universal Testing Machine and testing was performed at room temperature. The initial gauge length L_0 and thickness of 10 mm and 6 mm, respectively, were prepared for testing. The testing was performed with a speed of 5 mm/min with a load cell of 500 N. The thermal stability of the nanocomposites sample was analyzed with Mettler Toledo Thermogravimetric Analyzer, Perkin Elmer STA 6000. The TGA analysis was performed with a heating rate of 20 °C/min from 30 to 900 °C by using a nitrogen gas flow of 50 cm/min. Each testing was repeated three times and the obtained values were noted for further analysis and discussion.

3. Results and discussion

3.1. Scanning electron microscopy

The scanning electron microscope analysis explored the core-shell structure of CS/CNWs/f-MWCNTs and CS/CNWs/Un-MWCNTs. As a neat chitosan and CS/CNWs-5% had been analyzed to compare the structure with modified nanocomposites. The SEM image in Fig. 1 (i) shows a smooth surface with some scratch look indicated a good dissolution of chitosan in acetic aqueous solution and formed a chitosan nanocomposite film (Qian and Yang, 2006; Jung et al., 2007). In short, Fig. 1 (ii) show a disorganized and some fractured look surface structure which indicates the presence of CNWs in chitosan matrix

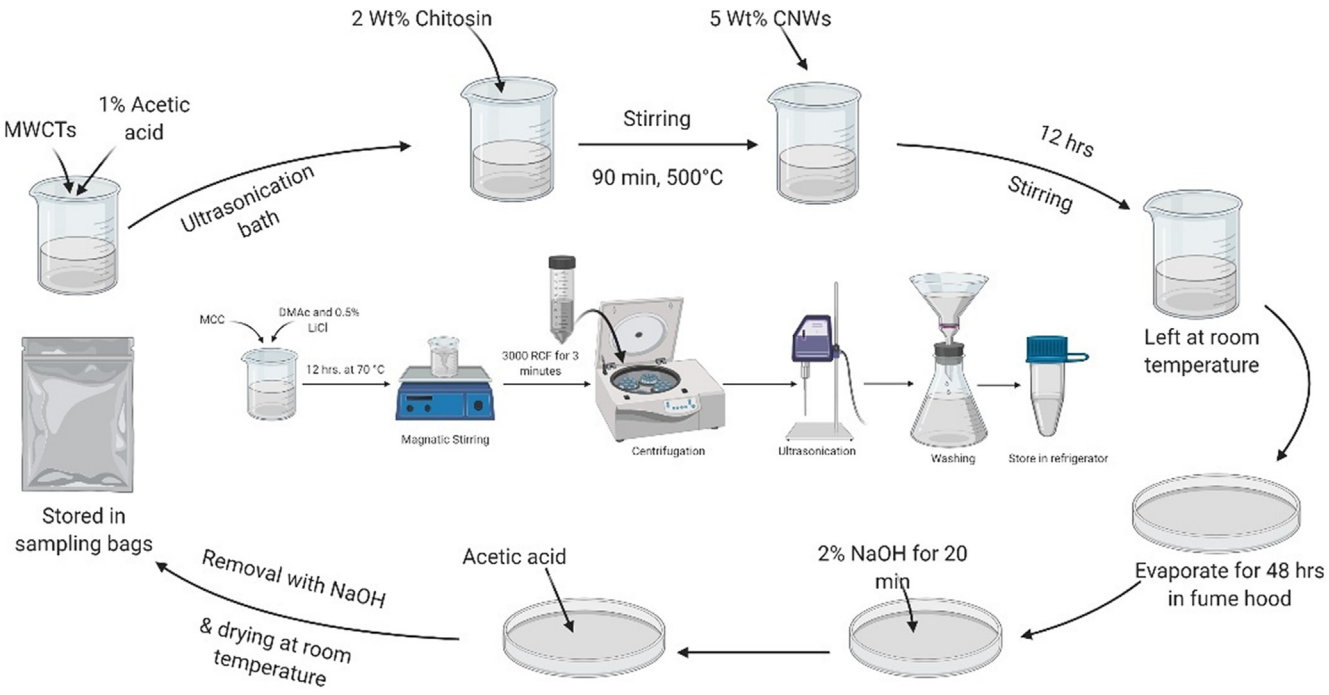

Fig. 1 Schematic Illustration of Preparation of CS/CNWs/MWCNTs Nanocomposites.

(Tanjung et al., 2017). The high aspect ratio and strong intermolecular hydrogen bonding of CNWs formed the aggregation with chitosan matrix (Akhlaghi et al., 2013). There were no large or unequal aggregates observed in the chitosan matrix which indicates that CNWs are well dispersed in this matrix. Meanwhile, upon fracturing, most of the CNWs got broken and then embedded instead of separated out of the matrix. It is most likely with the results of the strong interfacial adhesion between the nanofiller and matrix. Consequently, the properties and performance of chitosan nanocomposite would directly be affected by the uniform dispersion of nanofiller in the chitosan matrix. Therefore, it correlates with the mechanical properties analysis which means that the addition of 5 wt % CNWs on the chitosan would improve or alter the tensile strength and Young's Modulus (Tanjung et al., 2017).

As studied in literature review, the chitosan matrix was highly insoluble in alkaline and natural organic solvents while well dissolved in acid aqueous solvent solution (pH $<$ 6). The amino group of chitosan would be protonated during the dissolution with the acetic acid aqueous solution and resulting as a polycation. On the other hand, the acid oxidation functionalized MWCNTs had the carboxylic acid groups at the sidewalls and end of the structure which present the negative charge. The preparation of chitosan, CNWs and MWCNTs were well mixed by ultra-sonication and magnetic stirrer where the chitosan matrix would absorb the CNWs and MWCNTs on the surface at certain molecular level by electrostatic interaction which resisted the MWCNTs and CNWs aggregation and formed a dark grey solution (Qian and Yang, 2006). From FESEM micrographs, it is easy to distinguish between MWCNTs and CNWs due to both differences in fibrous shape. The CNWs are present as disorganized fracture look while the MWCNTs were in network or threadlike (Liu et al., 2005). The MWCNTs were easy to aggregate during the evaporation process through the π bond interaction and high surface specific area. In the meantime, the evaporation of water solvent could strengthen the agglomeration of nanowhiskers (Liu et al., 2016). The SEM images obviously shows that the homogeneous dispersion of MWCNTs in CS/CNWs-5% is significantly improved probably by the Van der Waals forces between CS/CNWs and surface of MWCNTs (Xue et al., 2017). This appearance shows a strong interfacial adhesion between CS/CNWs and MWCNTs. This strong bonding between CS/CNWs and MWCNTs help to improve the mechanical properties of nanocomposites. With the presence of a functional group of chitosan, CNWs and MWCNTs would form a laminated film with sufficient tensile strength but ductile nanocomposite films (Tanjung et al., 2017). In both SEM images for CS/CNWs/f-MWCNTs in Fig. 1 (iv) and CS/CNWs/Un-MWCNTs in Fig. 1 (iv) clearly show a quite similar micrograph which indicates Un-MWCNTs also capable to well disperse in CS/CNW-5% and formed a nanocomposites film where no agglomerations were observed. Therefore, FESEM shown that CS/CNWs/f-MWCNTs and CS/CNWs/Un-MWCNTs nanocomposite films were successfully synthesized with the presence of each chitosan, CNWs and MWCNTs. In the overall observation, the presence of CNWs and MWCNTs clearly alternate the surface morphology while the Un-MWCNTs and f-MWCNTs leading to form a slightly different morphology, corresponding with different mechanical properties and degree of crystallinity (Tanjung et al., 2017).

3.2. Fourier-transform Infrared Spectroscopy

The FTIR analysis is performed in the range of 400–4000 cm^{-1} to determine the presence of functional groups in the nanocomposites films. As the neat CS and CS/CNW-5% has been analyzed to determine the possible presence of functional groups before going through the analysis for characteristic peak for CS/CNWs/f-MWCNTs and CS/CNWs/Un-

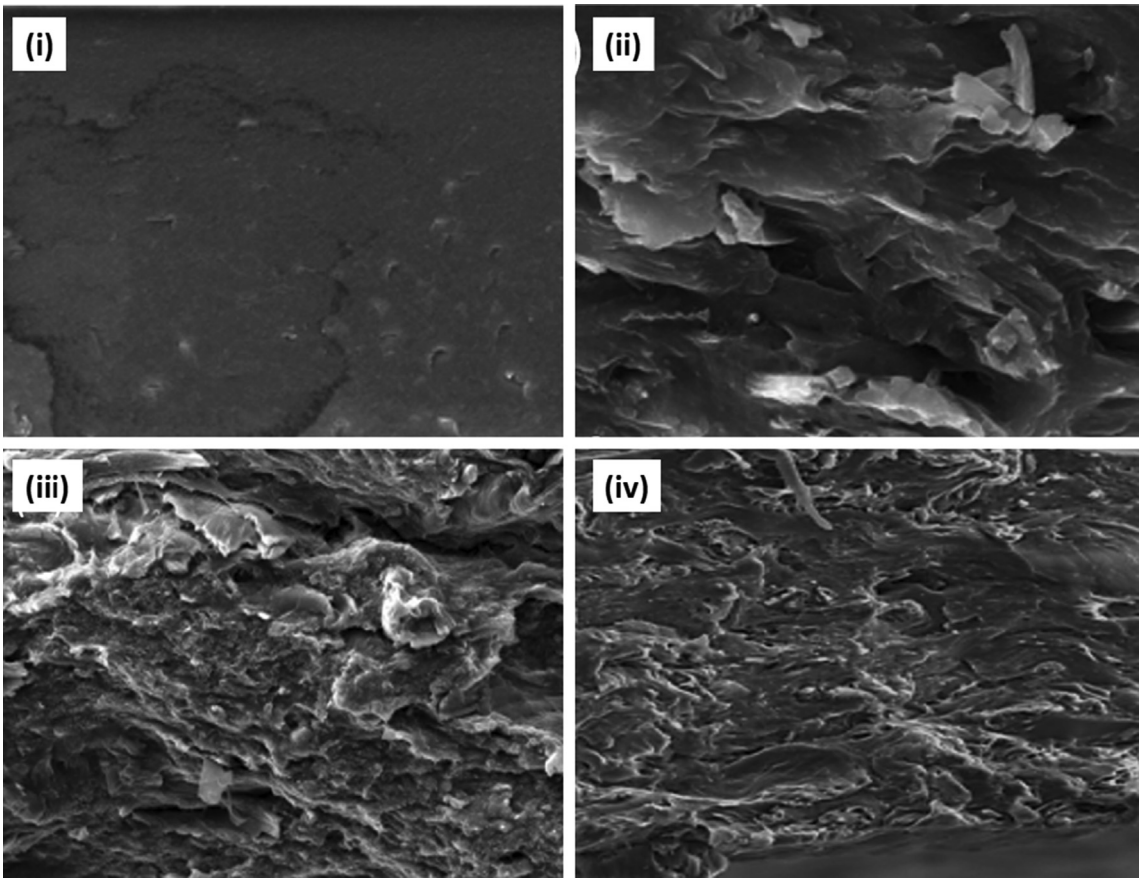

Fig. 2 FESEM micrographs of CS (i) CS/CNW (ii) CS/CNW/Un-MWCNTs (iii) and CS/CNW/*f*-MWCNTs (iv) nanocomposites at 20 μm.

MWCNTs. The neat chitosan in Fig. 2 (i) shows the —OH peak which the stretching vibration presence from 3200 to 3600 cm^{-1} and the intramolecular hydrogen bonds, peak at 2880 cm^{-1} indicate as CH. The presence of N-acetyl groups confirmed at the band around 1657 cm^{-1}, C—N stretching amide at around 1365 cm^{-1} and the peak at 1594 cm^{-1} due to the bending vibration of N—H, respectively. The stretching vibration band around 1058 cm^{-1} represent as C—O—C bridge [β (1, 4) glyosidic bonds]. This analysis has an agreement with the several studies (Fernandes Queiroz et al., 2014; Abo Elseoud et al., 2018; Venugopal et al., 2016; Marques Neto et al., 2019). On the other hand, Fig. 2 (ii) shows the modified chitosan with CNWs. Chitosan and CNWs consists of almost similar spectrum characteristic peaks. In short, the CS/CNWs nanocomposite film show the characteristic peak as C═O stretching (amide I bands) would present at 1500–1750 cm^{-1}, the 1500–1600 cm^{-1} would attribute as C—N stretching vibration (amide II bands) and N—H bending as the characteristic peaks for chitosan composites. The peak at 1161 and 1026 cm^{-1} indicate CS/CNWs nanocomposite as saccharide structure and represent as C—O—C bridge [β (1, 4) glyosidic bonds]. The presence of stretching vibration at 1200–1700 cm^{-1} indicates that the strong hydrogen bonds interaction via between functional groups of CNWs and chitosan which lead to a formation of the transparent nanocomposites film surface. The peak at 3200–3600 cm^{-1} had become deeper which suggested the presences of same functional groups and strong interaction of sulphate functional groups of CNWs surface with $—NH_2$ functional groups of chitosan. This analysis indicated that CNWs were physically modified into the chitosan matrix by solution casting method. These characteristic peak results show agreement with several studies (Tanjung et al., 2017; Abo Elseoud et al., 2018; Geng et al., 2015). Fig. 2 (iii) shows the comparison of FTIR characteristic peaks of CS/CNWs/f-MWCNTs and CS/CNWs/Un-MWCNTs which displayed slightly different characteristic peaks. The characteristic peaks for 3200–3630 cm^{-1} attributed to the stretching vibration of —OH overlapped with —NH stretching due to the intermolecular hydrogen bond for the polysaccharide of chitosan matrix. A peak at 2908 cm^{-1} appeared due to the presence of CH_2 stretch of the CNWs composites. A peak observed at 1661 cm^{-1} for both CS/CNWs/f-MWCNTs and CS/CNWs/Un-MWCNTs due to the presence of C═C stretching of MWCNTs, the peak at 1598 cm^{-1} was due the C═O stretching amide I of chitosan, the band stretching vibration around 1038 cm^{-1} represent the C—O—C bridge [β (1, 4) glyosidic bonds]. Comparative to neat chitosan, the C═O functional group is slightly shifted from 1653 cm^{-1} to 1598 cm^{-1} due to the network of intermolecular hydrogen bonds between MWCNTs with CS/CNWs (Choi et al., 2019). As clearly observed that the peak vibration for the CS/CNWs/Un-MWCNTs nanocomposite film is smaller than CS/CNWs/f-MWCNTs. It is most likely due to the lack of functional group in the Un-MWCNTs. There is a deformation

of primary amine N—H stretching observed compared to neat chitosan which was shifted from 1594 cm^{-1} to 1440 cm^{-1} due to the interaction between the amine group of chitosan and functional groups of carbon nanotubes (Carson et al., 2009). The overall band at 1400–1650 cm^{-1} for CS/CNWs/f-MWCNTs indicated the presence of carboxylic group of v (COOH) of functionalized MWCNTs which reacts with the amino functional group of chitosan during modification and converted into amide (—CONH—) group (Venkatesan et al., 2012). However, in CS/CNWs/Un-MWCNTs there is hard to analyze the primary amine N—H stretching and the section on 1600 cm^{-1} till 400 cm^{-1}. It is most likely due to lack of functional group in Un-MWCNTs and had a defect to the structure of CS/CNWs during physical modification. Overall results indicated that the CNWs and f-MWCNTs are well dispersed and integrated into chitosan matrix during solution casting technique. However, the Un-MWCNTs also consider well dispersed while there is lack of intermolecular interaction with the CS/CNWs which clearly observed in FTIR analysis.

3.3. Energy-dispersive X-ray Spectroscopy (EDS)

The elemental weight % of the chemical composites were analyzed with EDS analysis and all the samples i.e. neat chitosan, CS/CNWs-5%, CS/CNWs/f-MWCNTs and CS/CNWs/Un-MWCNTs did not presented any impurity as assumed from Fig. 3 (i-iv). Based on the results, the CS/CNWs/f-MWCNTs had higher oxygen content as compare to CS/CNWs/Un-MWCNTs. It could be explained that the acid functionalized MWCNTs consist of oxygenated functional group, whereby verified that the untreated MWCNTs lack of this functional group (Jun et al., 2018). Besides, CS/CNWs/f-MWCNTs and CS/CNWs/Un-MWCNTs had a higher carbon content compare to neat chitosan and CS/CNWs. The increase of carbon contents could state that both f-MWCNTs and Un-MWCNTs was well-dispersed in the CS/CNWs and directly increase on carbon contents in the nanocomposites.

On the other hand, nitrogen was only detected in CS/CNWs/f-MWCNTs nanocomposite due to the reaction between dialdehyde and amino group during solution casting modification (Xu et al., 2019). Furthermore, the oxygen content of the CS/CNWs, CS/CNWs/f-MWCNTs and CS/CNWs/Un-MWCNTs was decreased compared to neat chitosan. The estimated results are also enlisted in Table 1. So, the supporting information provided from EDS analysis shows that both f-MWCNTs and Un-MWCNTs is well attached and well dispersed with CS/CNWs-5%.

3.4. Mechanical properties

The mechanical properties were studied on the tensile strength (TS), Young's modulus (YM) and elongation break (EB%) of nanocomposites at room temperature. The mechanical properties of a neat chitosan matrix were poor with TS 21.6 ± MPa which similar to reported one (Corsello et al., 2017; Rong et al., 2017). The data in Table 2 confers that with 5% concentration of CNWs, the EB (%) only had a slight change from 13.5% to 12.5%. However, tensile strength and modulus were increases to 22.5 MPa and 402.5 MPa compared to neat CS. It is because CS is inherently hydrophilic in nature and a very polar matrix which can easily aggregate with CNWs (Corsello et al., 2017; Rong et al., 2017; Li et al., 2009). Moreover, CNWs could homogeneously have dispersed in the chitosan polymer matrix. However, it was difficult to have a well-dispersed CNWs with a concentration higher than 5% due to the high weight percentage of nanofiller suspension that can deteriorate the homogeneity of Chitosan/acetic acid/CNWs system (Geng et al., 2015). Consequently, 5 wt% of CNWs was chosen as the best ratio for CS/CNWs nanocomposite and used for further study.

Fig. 4 (i) showed the effect of different concentration of Un-MWCNTs and f-MWCNTs on the tensile strength of CS/CNWs nanocomposites films. A comparative study had been performed by using the Un-MWCNTs and f-MWCNTs as an additional nanofiller. The effect of Young's Modulus and Elongation Break vs concentration is shown in Fig. 4 (ii) and (iii) respectively. The results shown in Table 2 show that with the presence of additional nanofiller the Tensile strength (TS) and Young's Modulus (YM) got significant improvement but Elongation break (EB) was decreased. Decrease in EB% can be supported by the various study as with the increasing of nanofiller would impart the stiffness effect to the nanocomposites which decrease the deformability of CS/CNWs nanocomposites films (Li et al., 2009; Yao Rong et al., 2017). Moreover, with the increase in loading of Un-MWCNTs and f-MWCNTs, the TS and YM of CS/CNWs film were increased.

By adding 0.5% f-MWCNTs to CS/CNWs the TS and YM were increased by about 70% (from 22.5 MPa to 38.25 MPa)

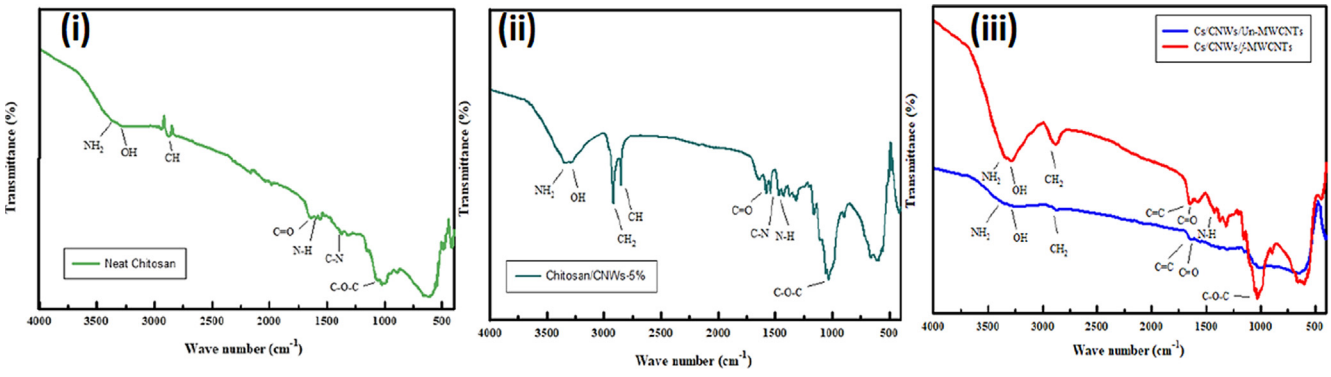

Fig. 3 FTIR spectra of Neat Chitosan (i) FTIR spectra of Chitosan/CNWs-5% (ii) and FTIR spectra of CS/CNWs/Un-MWCNTs (blue) and CS/CNWs/f-MWCNTs (red) (iii).

Table 1 Chemical composition of nanocomposite films.

Elemental composition	Neat chitosan	CS/CNW-5%	CS/CNWs/f-MWCNTs	CS/CNWs/Un-MWCNTs
C	55.63	55.92	60.99	69.33
O	44.37	44.08	36.34	30.67
N	–	–	2.67	–

Table 2 Mechanical properties of CS/CNWs/MWCNTs composites with addition of different concentration of CNWs, Un-MWCNTs and f-MWCNTs into neat CS.

CNWs concentration (%)	MWCNTs concentration (%)	Tensile strength (MPa)	Elongation at break (%)	Young modulus (MPa)
CS/CNWs/Un-MWCNTs				
0	0	21.6	13.5	399.5
5	0	22.5	12.5	402.5
5	0.1	28.67	10.53	495.6
5	0.3	30.54	8.65	524.6
5	0.5	31.25	7.98	535.76
CS/CNWs/*f*-MWCNTs				
0	0	21.6	13.5	399.5
5	0	22.5	12.5	402.5
5	0.1	35.1	8.234	523.25
5	0.3	37.354	7.468	623.83
5	0.5	38.25	6.99	644

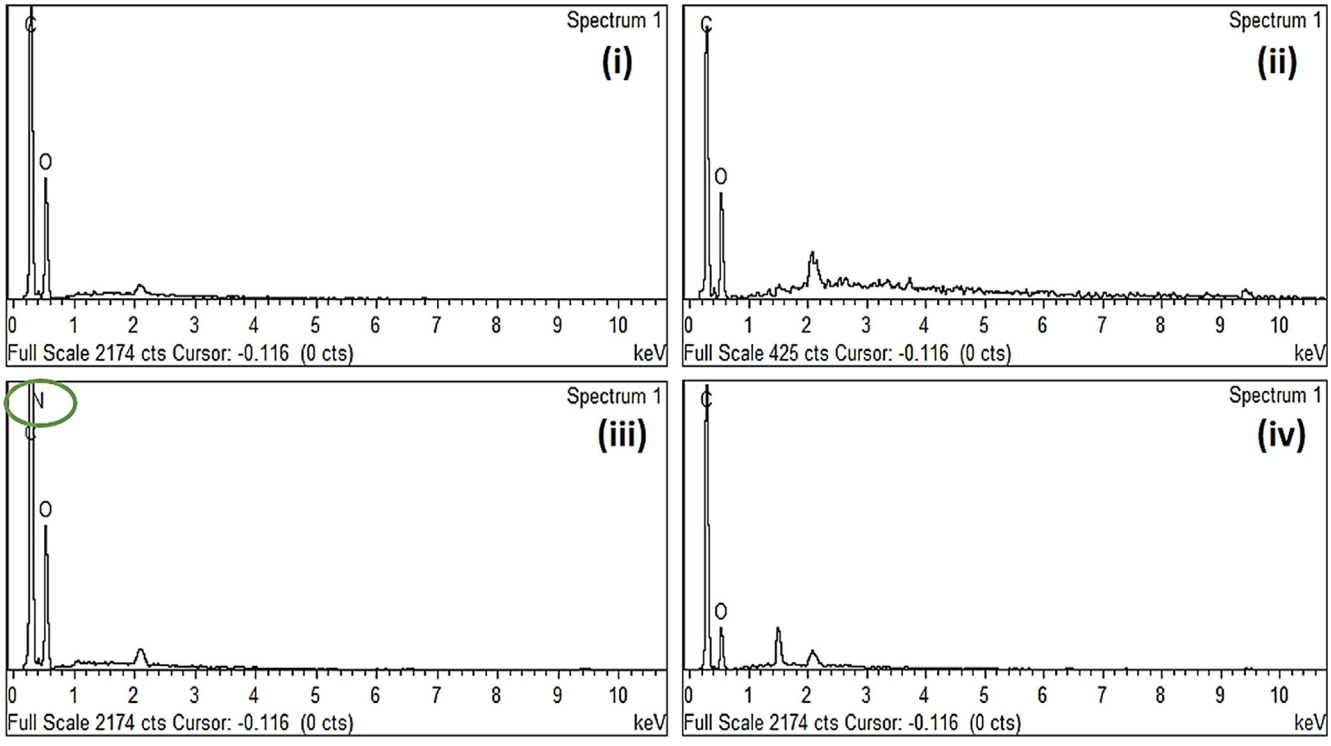

Fig. 4 EDS spectra of CS (i), CS/CNWs (ii), CS/CNWs/f-MWCNTs (iii) and CS/CNWs/Un-MWCNT (iv) composite films.

and 60% (402.5 MPa to 644 MPa) respectively, but decrease the EB by 44.08% (12.5–6.99%). However, an addition of 0.5% Un-MWCNTs, the TS and YM gave rise for about 39% (22.5 MPa to 31.25 MPa) and 21% (402.5 MPa to 535.76 MPa) respectively and decrease the EB approximately 36.2% (12.5–7.98%). As the overall significant perceived from the results is that the addition of 0.1% of MWCNTs had drastically enhanced the mechanical properties of CS/CNWs film. However, with the further increase for nanofiller aggregation at higher concentration of MWCNTs, the mechanical properties observed in Table 2 only increased slightly. With a higher concentration additional nanofillers, it was hard to completely

well disperse in CS/CNWs solution due to the strong internal Van der Waal force and the high viscosity of chitosan solution. Other than that, a low weight percent of chitosan matrix which dissolved in acetic acid unable to contribute incorporation for a high amount of nanofiller reinforcement.

Significantly, it is perceived that the addition of Un-MWCNTs to CS/CNWs experienced lower mechanical properties as compared to the f-MWCNTs. Nevertheless, both f-MWCNTs and Un-MWCNTs are capable to be dispersed in a 1% acetic acid aqueous solution. An acid functionalized MWCNTs would present with a number of the hydrophilic group such as —OH and —COOH group along their backbone and lead to overcome the strong internal Van der Waal force interaction (Rong et al., 2017; Shang et al., 2013). The presence with poor or unequal dispersion and solubility of nanofiller in the CS/CNWs matrix would lead to inequivalent enhancement for the properties of nanocomposites. A f-MWCNTs with no sign of structure devastation as a nanofiller well-dispersed with CS/CNWs nanocomposites film might obtain with a slightly different mechanical properties results (Shang et al., 2013; Wang et al., 2005; Sun et al., 2011). Other than that, an improvement of mechanical properties for a CS/CNWs with Un-MWCNTs as nanofiller had the agreement with the study reported by (Aryaei et al., 2014). The observation of mechanical properties could be supported by previous researches which performed chitosan matrix modified with MWCNTs (Wang et al., 2005; Aryaei et al., 2014). Chitosan is a very polar and inherent hydrophilic matrix which could be modified with two nanofillers and enhanced its mechanical properties. Therefore, it can be explained that the addition of two nanofillers had extended to a formation of percolate network within the chitosan matrix (Amri et al., 2013). As this distinctly results with forming a stronger intra and inter hydrogen bonding between nanofillers and chitosan matrix which facilitated the formation of a rigid interface (Lewandowska, 2015). The overall increment for mechanical properties can be attributed to the interaction of both f-MWCNTs and Un-MWCNTs as extra nanofiller with CS/CNWs. Suggestively, the result represents a strong interaction of CS/CNWs with the Un-MWCNTs and f-MWCNTs, the YM and TS would increase as the extra energy was needed to overcome the intra and inter molecular bonding energy.

3.5. Thermogravimetric analysis

Thermogravimetric analysis was performed to analyze the thermal behavior of the modified nanocomposites. As for the comparative study, the chitosan/CNWs-5% had been modified with f-MWCNTs and Un-MWCNTs. The thermal analysis in Fig. 5 (I and ii) has shown three distinct weight loss for CS/CNWs/

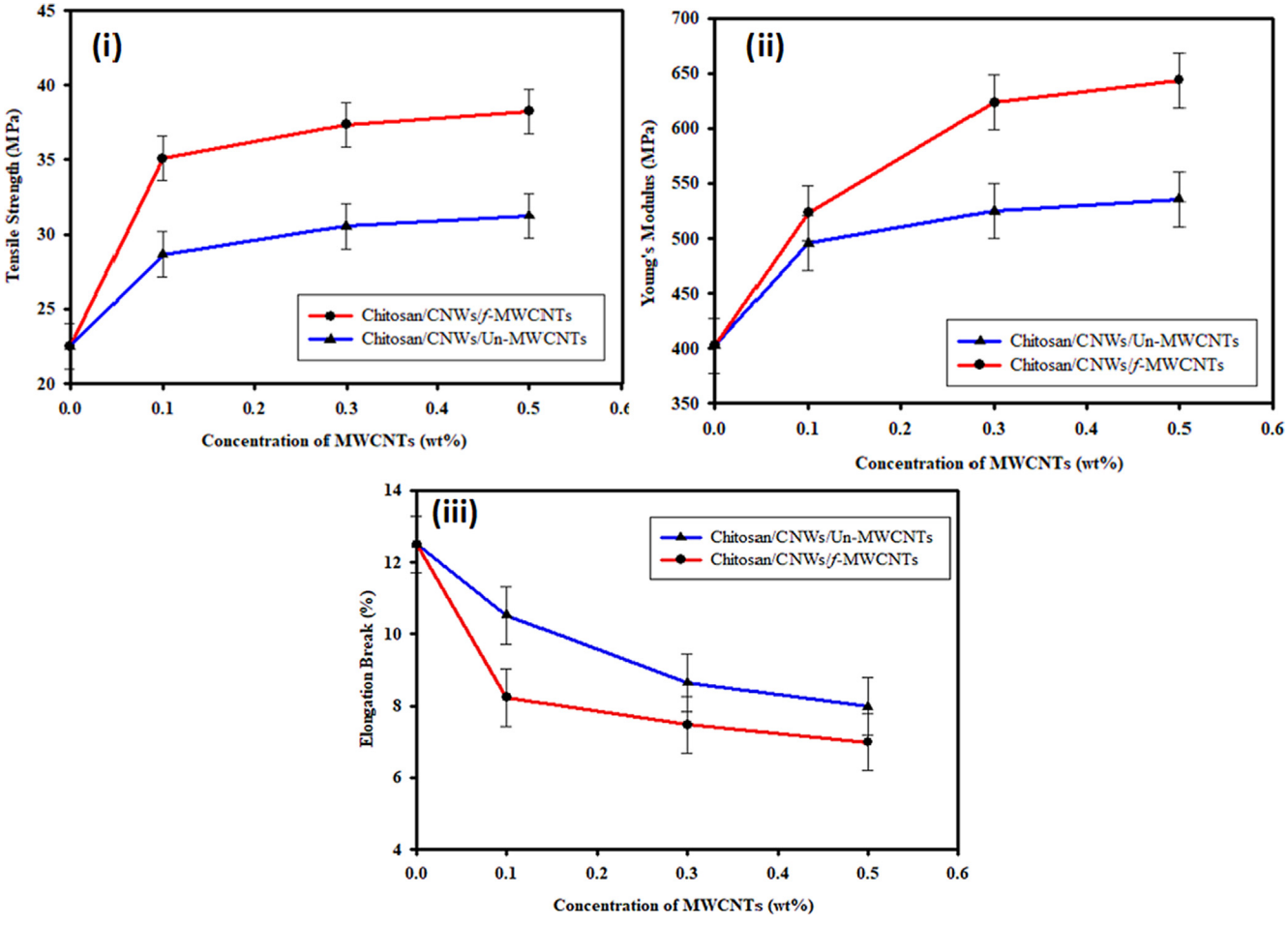

Fig. 5 Dependence of TS (i), YM (ii) and EB (%) (iii) upon concentration of MWCNTs on Chitosan/CNWs Nanocomposite Films.

Un-MWCNTs and four for CS/CNWs/f-MWCNTs respectively. The first stage showed a minor weight loss of about 4% at 50.6 °C for CS/CNWs/Un-MWCNTs and 64.5 °C for CS/CNWs/f-MWCNTs which was signified to the evaporation of water vapors (Venugopal et al., 2016; Yu et al., 2009). While nanocomposite films sample undergo preparation, the samples had been left in fume hood for 72 hrs. with the purpose of removing the water vapors and solvent, then kept in a close zip bag. However, there might be some water vapors physically absorbed to the surface of nanocomposites during testing preparation. In the second stage, a long range of decomposition for weight loss occur at 380 °C about 7.8% for CS/CNWs/f-MWCNTs and around 5.6% for CS/CNWs/Un-MWCNTs which started at 475 °C and most likely due to the chitosan matrix involved a minor depolymerization or decomposition of glucosamine, amino side and N-acetyl side groups (Shawky et al., 2012). The third stage undergone minor weight loss of about 0.8% for the CS/CNWs/f-MWCNTs occurred at a temperature range of 536–751.4 °C. It was most likely attributed to the —COOH group of f-MWCNTs which had damaged the surface of the chitosan matrix or due to the defect on f-MWCNTs structure during acid oxidation and affect the nanocomposite (Jun et al., 2018; Carson et al., 2009). Lastly, a sharp weight loss region from 751 °C to 838 °C for CS/CNWs/f-MWCNTs and 638 °C to 837 °C for CS/CNWs/Un-MWCNTs was observed which might be ascribed for the thermal degradation of chitosan polymer. Compared to the study performed by (Rong et al., 2017), the neat chitosan and CS/CNW-5% would have a sharp weight lost at 250 °C and 350 °C, respectively (see Fig. 6).

However, this research indicated that the addition of f-MWCNTs and Un-MWCNTs would prevent or delay the degradation of CNWs remarkably and the addition of CNWs together with MWCNTs had a more strong interaction with chitosan matrix leading to more effective and enhanced thermal stability of chitosan matrix (Liu et al., 2016; Carson et al., 2009; Celebi and Kurt, 2015). The overall degradation of CS/CNWs/Un-MWCNTs nanocomposites film showed almost similar behavior to CS/CNWs/f-MWCNTs which indicates that the Un-MWCNTs also enable to be well dispersed in chitosan matrix (Liu et al., 2016). It is most likely due to the

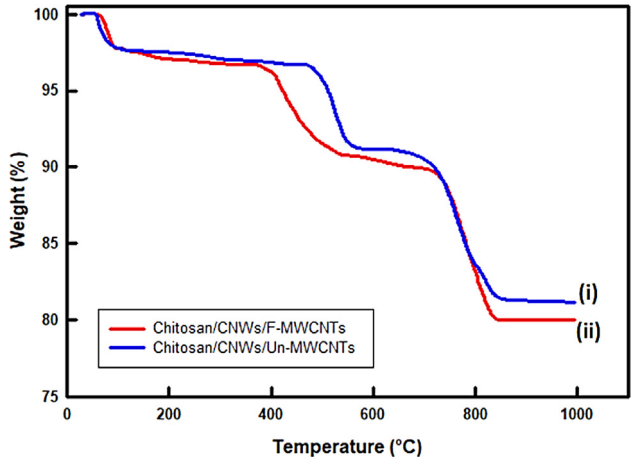

Fig. 6 TGA analysis of CS/CNWs/Un-MWCNTs (i) and CS/CNWs/f-MWCNTs (ii) composite films.

received Un-MWCNTs was in high purity by little or absence of any sites defect (Carson et al., 2009). Therefore, the extended results showed that the f-MWCNTs had a higher increment on the thermal stability of CS/CNWs as compare to Un-MWCNTs.

4. Conclusion

The main objective of the present research was to investigate the comparative analysis of reinforcement of f-MWCNTs and Un-MWCNTs on CS/CNWs matrix with respect to modifications in its structure, physical characteristics, mechanical and thermal properties. The experiment revealed that both f-MWCNTs and Un-MWCNTs were well-dispersed in CS/CNWs aqueous solution. Analytical characterizations showed that presence of MWCNTs on the CS/CNWs would clearly alternate the surface morphology and indicated that both MWCNTs were well-dispersed in CS/CNWs. Referring with mechanical viewpoint, the chitosan with 5% of CNWs shown the TS, YM and EB of 22.5 MPa, 402.5 MPa and 12.5%, respectively. However, the reinforcement of CS/CNWs nanocomposites film with MWCNTs experienced a significant improvement in mechanical properties and also increased the thermal stability by delaying the degradation of CS/CNWs. Both the f-MWCNTs and Un-MWCNTs have significantly reinforced the CS/CNWs composite providing the improved mechanical and thermal properties. However, CS/CNWs/ *f*-MWCNTs displayed much upgraded and more enhanced characteristics comparative to CS/CNWs/Un-MWCNTs. Thus, the analysis of the possible effects addition of MWCNTs on CS/CNWs nanocomposites to the structure morphology, mechanical and thermal properties had been achieved and well explained. Hence, the outcome of the research could provide extensive significance of chitosan-based composites providing excellent mechanical and thermal properties leading to the possibility of their applications in food packaging and preservation, pharmaceutics, wastewater and water treatment, biotechnology and agriculture.

Declaration of Competing Interest

The authors declare that they have no known competing financial interests or personal relationships that could have appeared to influence the work reported in this paper.

Acknowledgments

We are very thankful to the Department of Chemical Engineering, Faculty of Engineering and Science, Curtin University for laboratory support. National Natural Science Foundation of China (NSFC) Grant No. 51950410596 and QNJ20200214011. This work was funded by the Researchers Supporting Project Number (RSP-2020/254) King Saud University, Riyadh, Saudi Arabia.

References

Abo Elseoud, W.S., et al., 2018. Chitosan nanoparticles/cellulose nanocrystals nanocomposites as a carrier system for the controlled release of repaglinide, vol. 111.

Abou El-Ela, R.M. et al, 2020. Interpenetrating Polymer Network (IPN) Nanoparticles for Drug Delivery Applications. In: Interpen-

etrating Polymer Network: Biomedical Applications. Springer, pp. 25–54.
Ahmad, A., Mubharak, N.M., Naseem, K., Tabassum, H., Rizwan, M., Najda, A., et al, 2020. Recent advancement and development of chitin and chitosan-based nanocomposite for drug delivery: Critical approach to clinical research. Arab. J. Chem 13, 8935–8964.
Ahmad, A., Jini, D., Aravind, M., Parvathiraja, C., Ali, R., Kiyani, M. Z., Alothman, A., 2020. A novel study on synthesis of egg shell based activated carbon for degradation of methylene blue via photocatalysis. Arabian J. Chem. 13 (12), 8717–8722.
Akhlaghi, P., Berry, R.C., Tam, K., 2013. Surface modification of cellulose nanocrystal with chitosan oligosaccharide for drug delivery applications, vol. 20.
Amri, F., Husseinsyah, S., Hussin, K., 2013. Mechanical, morphological and thermal properties of chitosan filled polypropylene composites: The effect of binary modifying agents. Compos. A Appl. Sci. Manuf. 46, 89–95.
Aravind, M., Ahmad, A., Ahmad, I., Amalanathan, M., Naseem, K., Mary, S.M.M., et al, 2020. Critical green routing synthesis of silver NPs using jasmine flower extract for biological activities and photocatalytical degradation of methylene blue. J. Environ. Chem. Eng., 104877
Aryaei, A., Jayatissa, A.H., Jayasuriya, A.C., 2014. Mechanical and biological properties of chitosan/carbon nanotube nanocomposite films. J. Biomed. Mater. Res. A 102 (8), 2704–2712.
Asghari, F. et al, 2017. Biodegradable and biocompatible polymers for tissue engineering application: a review. Artif. Cells Nanomed. Biotechnol. 45 (2), 185–192.
Bao, Y. et al, 2018. Fabrication of cellulose nanowhiskers reinforced chitosan-xylan nanocomposite films with antibacterial and antioxidant activities. Carbohydr. Polym. 184, 66–73.
Carson, L. et al, 2009. Synthesis and characterization of chitosan–carbon nanotube composites. Mater. Lett. 63 (6), 617–620.
Celebi, H., Kurt, A., 2015. Effects of Processing on the Properties of Chitosan/Cellulose Nanocrystal Films 133, 284-293.
Choi, Y.-B. et al, 2019. The electrochemical glucose sensing based on the chitosan-carbon nanotube hybrid. Biochem. Eng. J. 144, 227–234.
Corsello, F.A. et al, 2017. Morphology and properties of neutralized chitosan-cellulose nanocrystals biocomposite films. Carbohydr. Polym. 156, 452–459.
Fernandes Queiroz, M., et al., 2014. Does the Use of Chitosan Contribute to Oxalate Kidney Stone Formation?, vol. 13, pp. 141-158.
Geng, C.-Z. et al, 2015. Mechanically reinforced chitosan/cellulose nanocrystals composites with good transparency and biocompatibility. Chin. J. Polym. Sci. 33 (1), 61–69.
Geng, C.-Z., et al., 2015. Mechanically Reinforced Chitosan/Cellulose Nanocrystals Composites with Good Transparency and Biocompatibility, vol. 33.
HPS, A.K. et al, 2016. A review on chitosan-cellulose blends and nanocellulose reinforced chitosan biocomposites: Properties and their applications. Carbohydr. Polym. 150, 216–226.
Hussain, S., Khan, A.J., Arshad, M., Javed, M.S., Ahmad, A., Shah, S.S.A., et al, 2020. Charge storage in binder-free 2D-hexagonal CoMoO4 nanosheets as a redox active material for pseudocapacitors. Ceram. Int.
Jun, L.Y. et al, 2018. Comparative study of acid functionalization of carbon nanotube via ultrasonic and reflux mechanism. J. Environ. Chem. Eng. 6 (5), 5889–5896.
Jung, Y.-J., et al., 2007. Preparation and Characterization of Chitosan/Cellulose Acetate Blend Film, vol. 19.
Kashif, M., Jaafar, E., Bhadja, P., Low, F.W., Sahari, S.K., Hussain, S., et al, 2020. Effect of Potassium Permanganate on Morphological, Structural and Electro-Optical Properties of Graphene Oxide Thin Films. Arabian J. Chem., 102953
Kashif, M., Ngaini, Z., Harry, A.V., Vekariya, R.L., Ahmad, A., Zuo, Z., et al, 2020. An experimental and DFT study on novel dyes incorporated with natural dyes on titanium dioxide (TiO2) towards solar cell application. Appl. Phys. A 126 (9), 1–13.
Kausar, A., 2017. Scientific potential of chitosan blending with different polymeric materials: A review. J. Plast. Film Sheeting 33 (4), 384–412.
Kijeńska, E. et al, 2016. Nanoengineered biocomposite tricomponent polymer based matrices for bone tissue engineering. Int. J. Polym. Mater. Polym. Biomater. 65 (16), 807–815.
Lewandowska, K., 2015. Characterization of chitosan composites with synthetic polymers and inorganic additives. Int. J. Biol. Macromol. 81, 159–164.
Li, H.-Z., Chen, S.-C., Wang, Y.-Z., 2015. Preparation and characterization of nanocomposites of polyvinyl alcohol/cellulose nanowhiskers/chitosan. Compos. Sci. Technol. 115, 60–65.
Li, Q., Zhou, J., Zhang, L., 2009. Structure and Properties of the Nanocomposite Films of Chitosan Reinforced with Cellulose Whiskers. Vol. 47, pp. 1069-1077.
Liu, Y. et al, 2016. Characterization and properties of transparent cellulose nanowhiskers-based graphene nanoplatelets/multi-walled carbon nanotubes films. Compos. A Appl. Sci. Manuf. 86, 77–86.
Liu, Y., et al., 2005. Decoration of carbon nanotubes with chitosan vol. 43, pp. 3178–80.
Marques Neto, J.D.O., Bellato, C.R., Silva, D.D.C., 2019. Iron oxide/carbon nanotubes/chitosan magnetic composite film for chromium species removal. Chemosphere 218, 391–401.
Melo, B.C. et al, 2018. Cellulose nanowhiskers improve the methylene blue adsorption capacity of chitosan-g-poly (acrylic acid) hydrogel. Carbohydr. Polym. 181, 358–367.
Mubarak, N.M. et al, 2014. Single stage production of carbon nanotubes using microwave technology. Diam. Relat. Mater. 48, 52–59.
Naseem, K., Zia Ur Rehman, M., Ahmad, A., Dubal, D., AlGarni, T. S., 2020. Plant Extract Induced Biogenic Preparation of Silver Nanoparticles and Their Potential as Catalyst for Degradation of Toxic Dyes. Coatings 10 (12), 1235.
Oksman, K. et al, 2006. Manufacturing process of cellulose whiskers/polylactic acid nanocomposites. Compos. Sci. Technol. 66 (15), 2776–2784.
Qian, L., Yang, X., 2006. Composite film of carbon nanotubes and chitosan for preparation of amperometric hydrogen peroxide biosensor. Talanta 68 (3), 721–727.
Rong, S.Y., Mubarak, N.M., Tanjung, F.A., 2017. Structure-property relationship of cellulose nanowhiskers reinforced chitosan biocomposite films. J. Environ. Chem. Eng. 5 (6), 6132–6136.
Saleem, M., Irfan, M., Tabassum, S., Alothman, Z., Javed, M.S., Hussain, S., et al, 2020. Experimental and Theoretical Study of Highly Porous Lignocellulose Assisted Metal Oxide Photoelectrodes for Dye-sensitized Solar Cells. Arabian J. Chem., 102937
Shang, S., Gan, L., Yuen, M.C.-W., 2013. Improvement of carbon nanotubes dispersion by chitosan salt and its application in silicone rubber. Compos. Sci. Technol. 86, 129–134.
Shawky, H.A., El-Aassar, A.H.M., Abo-Zeid, D.E., 2012. Chitosan/carbon nanotube composite beads: Preparation, characterization, and cost evaluation for mercury removal from wastewater of some industrial cities in Egypt. J. Appl. Polym. Sci. 125 (S1), E93–E101.
Shi, Z. et al, 1999. Mass-production of single-wall carbon nanotubes by arc discharge method. Carbon 37 (9), 1449–1453.
Sun, F. et al, 2011. Mechanical properties of multilayered chitosan/CNT nanocomposite films. Mater. Sci. Eng., A 528 (21), 6636–6641.
Tanjung, F.A. et al, 2017. Bilayer-Structured Regenerated Cellulose/Chitosan Films Prepared with Ionic. Liquid 17 (3), 9.
Thakur, V.K., Voicu, S.I., 2016. Recent advances in cellulose and chitosan based membranes for water purification: a concise review. Carbohydr. Polym. 146, 148–165.

Venkatesan, J. et al, 2012. Preparation and characterization of chitosan–carbon nanotube scaffolds for bone tissue engineering. Int. J. Biol. Macromol. 50 (2), 393–402.

Venugopal, G., et al., 2016. Nano-dynamic mechanical and thermal responses of single-walled carbon nanotubes reinforced polymer nanocomposite thin-films, vol. 688.

Wang, S.-F., et al., 2005. Preparation and Mechanical Properties of Chitosan/Carbon Nanotubes Composites 6, 3067-3072.

Wróblewska-Krepsztul, J. et al, 2018. Recent progress in biodegradable polymers and nanocomposite-based packaging materials for sustainable environment. Int. J. Polym. Anal. Charact. 23 (4), 383–395.

Xu, Q., et al., 2019. Fabrication of Cellulose Nanocrystal/Chitosan Hydrogel for Controlled Drug Release, vol. 9, 253.

Xue, B., et al., 2017. Functionalized multiwalled carbon nanotubes by loading phosphorylated chitosan: Preparation, characterization, and flame-retardant applications of polyethylene terephthalate vol. 30. 095400831773637.

Yao Rong, S., Mujawar, M., Tanjung, F., 2017. Structure-Property Relationship of Cellulose Nanowhiskers Reinforced Chitosan Biocomposite Films 5, 6132-6136.

Yu, J.G. et al, 2009. Rapid microwave synthesis of chitosan modified carbon nanotube composites. Int. J. Biol. Macromol. 44 (4), 316–319.

Zhan, M., Hussain, S., AlGarni, T.S., Shah, S., Liu, J., Zhang, X., et al, 2020. Facet controlled polyhedral ZIF-8 MOF nanostructures for excellent NO2 gas-sensing applications. Mater. Res. Bull. 136, 111133.

Zhang, X.Z., Xu, P.H., Liu, G.W., Ahmad, A., Chen, X.H., Zhu, Y. L., et al, 2020. Synthesis, characterization and wettability of Cu-Sn alloy on the Si-implanted 6H-SiC. Coatings 10 (9), 906.